The appearance of "blurred" digital images is a consequence of the violation of the immobility of the camera during the shooting of the objects under study. To this end, a procedure was devised for matched filtering of the blurred digital image of the object using its typical image form in a series of frames.

This procedure is based on the automated formation of a typical form of a digital image, as well as on the choice of special parameters for the transfer function of the matched filter. Adapting the procedure specifically to the typical form makes it possible to perform a more accurate assessment of the required parameters of the blurred digital image compared to the analytically set profile.

The formation of a typical form makes it possible to take into account the features of the very formation of the blurred image on each frame of the original series. Based on this, a more accurate assessment of the initial approximation of the parameters of all Gaussians of the object image is performed. In practice, matched filtering makes it possible to highlight blurred images of objects against the background of substrate noise. Also, using the matched filtering procedure makes it possible to improve the segmentation of images of reference objects and reduce the number of false detections.

The devised procedure for the matched filtering of a blurred digital image using its typical form has been tested in practice as part of the research in the framework of the CoLiTec project. It was implemented in the intraframe processing unit of the Lemur software for the automated detection of new and tracking of known objects. Owing to the use of Lemur software and the proposed computational procedure introduced into it, more than 700,000 measurements of various objects under study were successfully processed and identified

Keywords: *image processing, blurred image, matched filter, transfer function, OLS-evaluation of parameters*

UDC 519.23: 004.932.4
DOI: 10.15587/1729-4061.2023.273674

DEVELOPMENT OF THE MATCHED FILTRATION OF A BLURRED DIGITAL IMAGE USING ITS TYPICAL FORM

Sergii Khlamov
Corresponding author
PhD, Test Automation Lead
SoftServe
Sadova str., 2D, Lviv, Ukraine, 79021
E-mail: sergii.khlamov@gmail.com
Vadym Savanevych
Doctor of Technical Sciences, Professor
Department of Systems Engineering**
Vladimir Vlasenko
PhD
Space Research and Communications Center***
Oleksandr Briukhovetskyi
PhD
Western Center of Radiotechnical Surveillance***
Tetiana Trunova
Engineer, Assistant*
Ihor Levykin
Doctor of Technical Sciences*
Viktoriia Shvedun
Doctor of Science in Public Administration, Professor,
Head of Scientific Department
Scientific Department of Management Problems in the Field of Civil Protection
National University of Civil Defence of Ukraine
Chernyshevska str., 94, Kharkiv, Ukraine, 61023
Iryna Tabakova
PhD, Associate Professor*
*Department of Media Systems and Technologies**
**Kharkiv National University of Radio Electronics
Nauky ave., 14, Kharkiv, Ukraine, 61166
***National Space Facilities Control and Test Center
Moskovska str., 8, Kyiv, Ukraine, 01010

Received date 09.12.2022
Accepted date 13.02.2023
Published date 28.02.2023

How to Cite: *Khlamov, S., Savanevych, V., Vlasenko, V., Briukhovetskyi, O., Trunova, T., Levykin, I., Shvedun, V., Tabakova, I. (2023). Development of the matched filtration of a blurred digital image using its typical form. Eastern-European Journal of Enterprise Technologies, 1 (9 (121)), 62–71. doi: https://doi.org/10.15587/1729-4061.2023.273674*

1. Introduction

Related to the issue of asteroid-comet danger [1], the leading direction for the use of astrometry [2] and photometry [3] methods is the automatic processing of the results of asteroid surveys. Huge astronomical catalogs [4] and archival big data [5] make it possible to accumulate, gain knowledge [6], and analyze accumulated data and measurements in the public domain [7] for the entire period of observation of specific celestial objects of the Solar System (SSO) [8].

However, the quality of conditions during filming directly proportionally affects the quality of SSO images on the frames generated by the charge-coupled device (CCD) [9]. This applies both to old images from archival data when

Copyright © 2023, Authors. This is an open access article under the Creative Commons CC BY license

CCD matrices were of lower resolution and quality and to freshly formed frames, during the formation of which the shooting conditions were violated. A similar effect on the shooting conditions can be exerted by an incorrectly chosen mode of telescope guidance, a mechanical failure of daily observation, a side wind, and the weather in general. This means that images of individual SSOs or of the entire frame/series of frames as a whole may be blurred. These unfavorable conditions significantly reduce the quality of detection of the objects under study using known computational methods.

Therefore, it is relevant to devise a procedure for the matched filtering of a blurred digital image of an object using its standard shape on a series of frames. This procedure will make it possible to more accurately assess the image parameters [10] of such "blurred" objects, which will allow them to be identified with those already known from the list of cataloged ones [4]. Also, this procedure improves the conditional probability of correct detection (CPCD) of real objects and reduces the number of false detections [11].

2. Literature review and problem statement

In the presence of significant synchronous displacements of all objects of a CCD frame for the entire time of exposure, such a CCD frame in the work is considered completely blurred. In this case, such a synchronous displacement cannot be neglected categorically. There is also a blur of images of SSOs (asteroids, meteors, comets) due to their natural motion. Such a blur is not considered in the work.

Various blurs or synchronous displacements of images of the objects under study on CCD frames affect the quality and accuracy of various imaging and machine vision tasks [12]. Namely, they affect the accuracy of detection and recognition of images of objects [13], parameter evaluation [14]. All of these methods are based on the analysis of only those pixels that potentially belong to the object under study. Their disadvantage is that when the image is blurred, it is completely impossible to initially identify specific pixels and reject those whose intensity exceeds the specified limit value [2, 15]. Paper [16] discusses the classification of images of various objects. It is based on machine learning and analytical models that have a preset classification and templates. The disadvantage of such a classification is that all templates have a clear typical shape and in the case of blurring the boundaries of the object image will not be recognized.

Works [17, 18] consider pixelation and segmentation of only point images of objects but it is not possible to process blurred images. The disadvantage of these methods is the impossibility of accurate processing of images of objects with an ambiguous number of brightness peaks.

Blurred images of objects affect the detection and evaluation of motion [10]. They also affect various methods for analyzing large data sets such as wavelet transformation (analysis) [19] and time series analysis [20]. The disadvantage of such methods is that they are adapted to work only with "pure" measurements, so blurred images will greatly spoil the overall indicator and give "outliers".

The disadvantage of the methods of frame addition [21] and machine vision [22] is the impossibility of application when the image of the object under study does not have clear boundaries on all CCD frames of the series. Other numerical methods that use the Hough, Radon transformations or their modifications [23, 24] are not able to detect the image of the object with the required CPCD under conditions of blurring of the image itself.

As practice shows, it is the matched filter that has the best efficiency in relation to CPCD [25]. It is a linear filter that minimizes the signal-to-noise ratio (SNR), thereby increasing the likelihood of detecting objects whose images have random additive noise with a normal Gaussian distribution embedded [26]. The method of matched filtering [27] is already known, but it uses an analytical image model. The main disadvantage of this method is the fact that the technique will not work correctly in the case when the image on different frames of the series is blurred differently.

Therefore, it is necessary to devise a procedure for the matched filtering of a blurred digital image of an object using its standard shape [28] on a series of frames.

3. The aim and objectives of the study

The aim of this study is to perform matched filtering of the blurred digital image of the object using its typical form on a series of frames. It is the formation of a typical image shape based on the frames of the original series that makes it possible to perform a more accurate assessment of the parameters compared to the analytically set profile.

To accomplish the aim, the following tasks have been set:

– to select single images of objects and form their rectangular areas with subsequent assessment of displacement and normalization;

– to form a typical form of the blurred image of the object and clarify it based on the frames in series;

– to determine the number of Gaussians of the obtained typical image of the object and estimate the initial approximation of the parameters of their form;

– to select the form and parameters of the transfer function of the matched filter with the subsequent evaluation of the image parameters;

– to devise a procedure for the matched filtering of the blurred digital image of the object using its typical form on a series of frames.

4. The study materials and methods

The object of our study is blurred digital images of various objects on CCD frames. Within the framework of this study, the main hypothesis was put forward that the use of matched filtering of the original blurred image would significantly increase the CPCD of objects. This can only be achieved if the devised method is used as a preliminary preparatory technique of image processing. Also, matched filtering will increase the accuracy of evaluating the parameters of objects when further performing the main tasks of image processing by already known methods.

The original data is a blurred digital frame A_{in} the size of $N_{CCDx} \times N_{CCDy}$. The image of the j-th object is really blurred, present on the frame, and is also in the area of intra-frame processing (AIFP), which is a set of Ω_{Nobj} pixels.

The obtained research results, as well as the devised method of matched filtering, were converted into a software code using the C++ programming language. This code was integrated into the system unit of intra-frame processing of the Lemur software package (Ukraine) [29] for the automat-

ed detection of new and tracking of known objects within the framework of the CoLiTec research project [30].

As an initial test information, various data obtained from different telescopes installed at observatories in Ukraine and the world were used. Namely, the ISON-Uzhgorod Observatory (Uzhgorod, Ukraine), the quantum optical system (QOS) "Sazhen-S" (Dunaivtsi, Ukraine), and the telescopes AZT8 (Dunaivtsi, Ukraine) and Takahashi BRC-250M (Uzhgorod, Ukraine); Mayaki Astronomical Observatory (Mayaki, Ukraine), the telescope OMT-800 [31]; Vihorlat Observatory (Humenné, Slovakia) [32]; National Astronomical Research Institute of Thailand (NARIT, Thailand) [33].

The observational conditions were specially selected so that the initial test series of CCD frames contained blurred images of the studied SSOs [8] of different standard shapes.

The devised computational method, implemented in the Lemur software package (Ukraine) as a pre-processing technique, assisted to the successful identification of more than 700,000 measurements of various SSOs. With this fact, the matched filtering method confirmed its practical significance within the framework of the main hypothesis put forward.

5. Results of studying the matched filtering of the blurred image using its typical form

5. 1. Selection of single images and formation of their rectangular areas, followed by bias estimation and normalization

On any blurred frame, there are single images of objects, which can have a completely different image shape from frame to frame in the series. Thus, in order to determine the typical shape of the image of a certain object on the entire frame, or the typical shape as the average of all objects in a series of frames, it is first necessary to select single images of all objects. Single blurred images of objects, especially during long exposure times, have the shape of a hill that stretches along the direction of their visible movement. A model is used in which the centers of all N_{segm} segments of the image lie on the same line. It passes through the anchor point of the blurred image of the j-th object with coordinates $x_{tj}\left(\Theta_{tj}^{over}\right)$ and $y_{tj}\left(\Theta_{tj}^{over}\right)$ at angle ω_j to the abscissa axis in the coordinate system (CS) of the frame. Θ_{tj}^{over} is the vector of the parameters of the blurred image of the j-th object.

To select single images, we form a list of bright images of objects. Next, it is ordered in ascending order of the shape parameter σ_{Gm}. This shape parameter is based on the shape parameters $\sigma_{Gm\ell}$ of each ℓ-th segment of the image from N_{segm} segments of Δx_{seg} pixels wide into which the image is split along the semi-major axis. This segmentation is carried out in the CS associated with the blurred image of the object itself where the center of the CS coincides with the center of the image itself. Thus, it is believed that all the pixels belonging to each segment also belong to the single image of the object itself. Next, the list of bright images excludes those images in which the σ_{Gm} shape parameter exceeds the median value of $\sigma_{G½}$ throughout the frame.

From the selected single images of objects Ω_{Sm}, a rectangular area of $N_{Sx}\times N_{Sy}$ pixels is formed. The size of such an area is determined by twice the sum of the maximum size of $N_{S\max x}$, $N_{S\max y}$ AIFP of the frame and the value of the border size N_{borx}, N_{bory} on the axis of abscissa and ordinate, respectively [27].

To obtain an average image of an object from selected single images, the offsets between those images are pre-calculated. Mutual bias is estimated relative to a single image of an object with maximum intra-frame correlation. The offset between the selected single images is calculated from the coordinates of the maximum linear correlation coefficient [34]. The value of the linear correlation coefficient of two single images of an object depends on their mutual displacement. The maximum coefficient is reached at the full combination of single images, and the maximum value characterizes the degree of linear similarity of the studied images.

To determine the typical shape of a single image of an object, it is necessary to normalize the resulting images. Normalization is necessary to eliminate differences in the aperture (PSF) brightness of object images when calculating the average or median of selected single images.

5. 2. Formation of a typical form of a blurred image of an object and its refinement based on the frames of the series

The typical form of the blurred image of the object on the frame is evaluated by N_{sel} pre-selected single images. For this purpose, a list of single images is formed with the aperture (total) brightness of the pixels of the objects' images $A_{\Sigma m}^{*}$, that satisfies the condition:

$$A_{\Sigma m}^{*} \geq (10 \div 20)\sigma_{noise}, \tag{1}$$

where σ_{noise} is a preliminary estimate of the standard deviation (RMS) of the brightness of the background of the frame;

$A_{\Sigma m}^{*} = \sum_{l=1}^{Nsm}\left(A_{l(i,k)m}^{*} - C_{fm}\right)$ is the aperture brightness of the pixels of the m-th single image of the object;

$A_{l(i,k)m}^{*}$ is the brightness of the l (i, k)-th pixel of the set Ω_{Sm} of the m-th single image of the object;

l (i, k) is the pixel number l in the set Ω_{Sm}, which is a function of the numbers of the ik-th pixel on the frame;

C_{fm} is the previously obtained average brightness value of the background of the frame.

For each single image, the eccentricity ε_m of the object image is calculated [35]:

$$\varepsilon_m = \frac{m_{20} + m_{02} - \sqrt{m_{20} - m_{02} + 4m_{11}^{2}}}{m_{20} + m_{02} + \sqrt{m_{20} - m_{02} + 4m_{11}^{2}}}, \tag{2}$$

where

$$m_{20} = \sum_{l=1}^{Nsm}\left(A_{l(i,k)m}^{*} - C_{fm}\right)\left(x_{l(i,k)m} - X_0\right)^2, \tag{3}$$

$$m_{02} = \sum_{l=1}^{Nsm}\left(A_{l(i,k)m}^{*} - C_{fm}\right)\left(y_{l(i,k)m} - Y_0\right)^2, \tag{4}$$

$$m_{11} = \sum_{l=1}^{Nsm}\left(A_{l(i,k)m}^{*} - C_{fm}\right)\left(y_{l(i,k)m} - Y_0\right)\left(x_{l(i,k)m} - X_0\right), \tag{5}$$

$$X_0 = \frac{\sum_{l=1}^{Nsm}\left(A_{l(i,k)m}^{*} - C_{fm}\right)x_{l(i,k)m}}{A_{\Sigma m}^{*}}, \tag{6}$$

$$Y_0 = \frac{\sum_{l=1}^{Nsm}\left(A_{l(i,k)m}^{*} - C_{fm}\right)y_{l(i,k)m}}{A_{\Sigma m}^{*}}, \tag{7}$$

m_{20}, m_{02}, m_{11} – second-order moments;

X_0 and Y_0 are first-order moments;

$x_{l(I,k)m}$, $y_{l(I,k)m}$ are the coordinates of the $l(i, k)$-th pixel of the m-th single image of the object.

Next, the length L_m of a single image of the object is calculated [28]. After that, single images of objects from the list are rejected. The rejection is based on a comparison with the following criteria:

– estimation of the eccentricity ε_m of a single image with a boundary allowable eccentricity value of γ_ε=0.6;

– estimation of the length L_m of a single image with a valid relative deviation of the length of the image of objects γ_L=0.1.

After this, a refined list of bright single images of objects is ordered in descending order of aperture brightness. The final step is to exclude 10÷20 % of images of objects with the highest brightness.

5. 3. Determination of the number of Gaussians of the obtained typical form and estimation of the initial approximation of the parameters

Each single blurred image can be represented by a certain number of Gaussians [28]. The number of Gaussians of a single image of the j-th object should be estimated separately from the Levenberg-Marquardt algorithm (ALM) [36]. The desired number of Gaussians N_{Gj} is selected from the range of values $\overline{N_{Gfirstj}, N_{Gendj}}$. Initial $N_{Gfirstj}$ and final N_{Gendj} values are determined based on the following parameters:

– the maximum size of the blurred image of the j-th object d_{conj}, which is equal to the maximum distance between two pixels belonging to the outline of the image of the j-th object;

– coefficients k_{first} and k_{end}, which set the minimum and maximum number of Gaussians, respectively;

– initial approximation of the Gaussian shape parameter σ_{Gj0} corresponding to the blurred image of the j-th object:

$$\sigma_{Gj0} = \frac{1}{N_{segj}} \sum_{m=0}^{N_{segj}-1} \sigma_{Gjm}. \qquad (8)$$

The desired number of Gaussians N_{Gjmin} of a single blurred image of the j-th object is chosen that at which the sum of the squares of deviations $F_{\Delta A\tau}\left(\Theta_{\tau jn}^{over}\right)$ is minimal. Next, the initial approximation of the gaussian shape parameters is estimated from the vector $\Theta_{\tau jn}^{over}$ of estimated parameters of a single blurred image of the j-th object. To do this, the sum of the squares of deviations between the experimental A_{ikj}^{*} and model $A_{Sikmj}(\Theta_{\sigma m})$ brightness of the pixels of the m-th segment of the single blurred image of the j-th object is applied to the ALM procedure [36]:

$$F_{\Delta A\sigma}\left(\Theta_{\sigma m}\right) = \sum_{k=\Omega_{segjm}} \left(A_{ikj}^{*} - A_{Sikmj}\left(\Theta_{\sigma m}\right)\right)^2 \underset{\Theta_{\sigma m}}{\rightarrow} \min, \qquad (9)$$

where $\Theta_{\sigma m}=(\sigma_{Gjm}, A_{Gjm}, y_{0jm})$ is the vector of estimated parameters of the m-th segment of the blurred image of the j-th object;

$A_{Sikmj}\left(\Theta_{\sigma m}\right) = A_{Gjm} \exp\left\{-\frac{1}{2\sigma_{Gjm}^2}\left[\left(y_{kj} - y_{0\,jm}\right)^2\right]\right\}$ is the model brightness of the pixels of the m-th segment of the blurred image of the j-th object;

σ_{Gjm} – estimates of the initial approximation of the gaussian shape parameter in the m-th segment;

A_{Gjm} – gaussian model amplitude in the m-th segment;

y_{0jm} is the coordinate of the reference center of the Gaussian in the m-th segment along the ordinate axis.

5. 4. Selecting the form and parameters of the matched filter transfer function and evaluating the image parameters

To select the form and parameters of the matched filter transfer function, it is necessary to determine the model brightness of each single blurred image obtained after the formation of a typical form.

The model brightness $A_{ik\tau j}\left(x_{ij}, y_{ij}, \Theta_{\tau j}^{over}\right)$ of the ik-th pixel for a single blurred image of the j-th object is determined by the following expression [27]:

$$A_{ik\tau j}\left(x_{ij}, y_{ij}, \Theta_{\tau j}^{over}\right) = C_j + \frac{A_{Gj}}{2\pi\sigma_{Gj}^2} \sum_{n=0}^{N_{Gj}-1} \exp\left\{-\frac{1}{2\sigma_{Gj}^2}\left[\left(x_{ij} - x_{\tau j}\left(\Theta_{\tau j}^{over}\right) - \ell_{nj}\cos\omega_j\right)^2 + \left(y_{ij} - y_{\tau j}\left(\Theta_{\tau j}^{over}\right) - \ell_{nj}\sin\omega_j\right)^2\right]\right\}, \qquad (10)$$

where C_j is the average brightness of the background substrate of a single blurred image of the j-th object;

x_{ij}, y_{ij} – coordinates of the ik-th pixel of the blurred image of the j-th object;

A_{Gj} is the model amplitude of gaussians corresponding to a single blurred image of the j-th object;

ℓ_{nj} is the position of the n-th Gaussian of N_{Gj} used to approximate a single blurred image of j-th objects.

It is also necessary to determine the spectrum of the resulting typical image, which is subject to matched filtering. It follows that the value of the uv harmonic of the discrete spectrum S_{uvj} of a single blurred image of the j-th object is determined by the following expression [37]:

$$S_{uvj} = A_{Gj} \exp\left[-2\pi^2\sigma_{Gj}^2\left(\left(\frac{u}{N_{CCDx}}\right)^2 + \left(\frac{v}{N_{CCDy}}\right)^2\right)\right] \times \sum_{n=0}^{N_{Gj}-1} \exp\left[i2\pi\left(u\frac{x_{\tau j}\left(\Theta_{\tau j}^{over}\right) + \ell_{nj}\cos\omega_j}{N_{CCDx}} + v\frac{y_{\tau j}\left(\Theta_{\tau j}^{over}\right) + \ell_{nj}\sin\omega_j}{N_{CCDy}}\right)\right], \qquad (11)$$

where $u = \overline{0, N_{CCDx}-1}$, $v = \overline{0, N_{CCDy}-1}$ are the harmonic numbers of the discrete spectrum of a single blurred image.

It is known that the transfer function H_{MF} of the matched filter is equal to the complex-conjugate spectrum S_{uvj}^{*} of the object image [25]. To ensure the position of the maximum response of the matched filter in the center of the blurred images of objects in the CS of the frame, it is necessary to set zero values for the coordinates of the image binding center [27]. Also, to match the aperture brightness of the pixels of the image of the j-th object on the original frame and on the frame after the matched filter, the complex-conjugate spectrum S_{uvj}^{*} is multiplied by its normalizing coefficient [38].

Thus, the H_{MF} transfer function of the matched filter for the entire single blurred image of the j-th object is as follows:

$$H_{FMuv}=\frac{1}{N_{Gj}}\exp\left[-2\pi^2\sigma_{Gj}^2\left(\left(\frac{u}{N_{CCDx}}\right)^2+\left(\frac{v}{N_{CCDy}}\right)^2\right)\right]\times$$
$$\times\sum_{n=0}^{N_{Gj}-1}\exp\left[-i2\pi\left(u\frac{\ell_{nj}\cos\omega_j}{N_{CCDx}}+v\frac{\ell_{nj}\sin\omega_j}{N_{CCDy}}\right)\right], \quad (12)$$

where H_{MFuv} is the uv harmonic of the transfer function of the matched filter.

After that, you need to evaluate the image parameters using the gaussian pixel model of the blurred image of the object. The quality criterion for assessing the parameters of the blurred image of the j-th object is the minimum sum of the squares of deviations between the experimental A_{ikj}^* and model $A_{ik\tau j}\left(\Theta_{\tau j}^{over}\right)$ brightness of the pixels of the blurred image of the j-th object:

$$F_{\Delta A\tau}\left(\Theta_{\tau j}^{over}\right)=\sum_{i,k=\Omega_{Nobj}}\left(A_{ikj}^*-A_{ik\tau j}\left(\Theta_{\tau j}^{over}\right)\right)^2\rightarrow\min_{\Theta_{\tau j}^{over}}, \quad (13)$$

where $\Theta_{\tau j}^{over}=\left(C_j,x_{\tau j}\left(\Theta_{\tau j}^{over}\right),y_{\tau j}\left(\Theta_{\tau j}^{over}\right),A_{Gj},\sigma_{Gj},\omega_j,d_j\right)$ is the vector of estimated parameters of the blurred image of the j-th object.

The estimated parameters of the image of the j-th object are:

– the average brightness of the background substrate C_j;

– position $x_{\tau j}\left(\Theta_{\tau j}^{over}\right)$, $y_{\tau j}\left(\Theta_{\tau j}^{over}\right)$;

– model amplitude of Gaussian A_{Gj};

– shape parameter σ_{Gj};

– the angle between the direction of the blur of the object image and the abscissa axis ω_j;

– the distance of movement of the object relative to the frame of the abscissa $d_j=\left(N_{Gj}-1\right)\sigma_{Gj}$.

To calculate all the parameters listed above from the vector of estimated parameters of the blurred image of the j-th object, it is necessary to submit the sum of the squares of deviations (13) to ALM [36].

5. 5. Procedure for the matched filtering of a blurred image using its typical form

The devised procedure for the matched filtering of the blurred digital image of the object using its typical form on a series of frames is a sequence of actions:

1. Select N_{sel} single blurred images of objects and form their rectangular areas with the subsequent calculation of linear correlation coefficients.

2. Determine offsets $N_{sel}-1$ of selected single blurred images of objects relative to a single image of an object with maximum intra-frame correlation.

3. Normalize N_{sel} selected single images of objects.

4. Form a list of single blurred images with the aperture (total) brightness of the pixels of the images of objects $A_{\Sigma m}^*$, in accordance with condition (1).

5. Calculate the eccentricity ε_m and the length L_m of each single blurred image of the object (2) based on the calculations of the moments of the second (3) to (5) and first (6), (7) orders.

6. Reject and refine the obtained single blurred images of objects from the list.

7. Determine the number of Gaussians N_{Gj} of each single image from a range of values $N_{Gfirstj},N_{Gendj}$.

8. Estimate the initial approximation of the gaussian shape parameters from the vector $\Theta_{\tau jn}^{over}$ of estimated parameters of each single blurred image using the ALM procedure (9).

9. Determine the model brightness $A_{ik\tau j}\left(x_{ij},y_{ij},\Theta_{\tau j}^{over}\right)$ of the ik pixel for a single blurred image of the j-th object using expression (10).

10. Determine the discrete spectrum S_{uvj} of a single blurred image of a j-th object using expression (11).

11. Determine the transfer function H_{MF} of the matched filter for a single blurred image of the j-th object according to expression (12).

12. Evaluate the parameters of the blurred image of the j-th object by feeding the sum of the squares of deviations (13) into ALM.

We studied the effectiveness of using a typical image of the object on the frames of the SAZHEN-S QOS (Dunaivtsi), and the telescopes AZT8 (Dunaevtsy), OMT-800 (Mayaki), and Takahashi BRC-250M (Uzhgorod). Below, Fig. 1–4, *a* show the typical examples of images blurred by the natural movement of objects found on the frames from these observatories. As well as images of a frame formed by the devised method of a typical form (Fig. 1–4, *b*) [28] and an analytical model of a blurred image of an object [27] (Fig. 1–4, *c*).

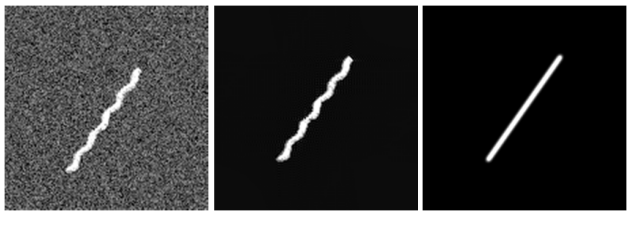

a *b* *c*

Fig. 1. Fragment of the frame of the telescope "Sazhen-S": *a* – the original image; *b* – the generated typical image; *c* – analytical image model

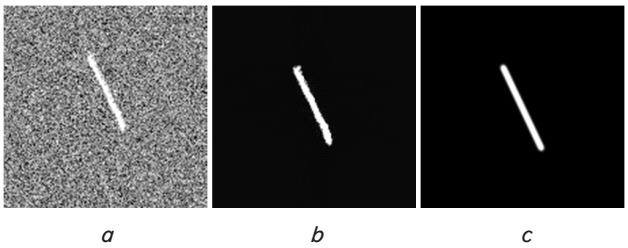

a *b* *c*

Fig. 2. Fragment of the frame of the OMT-800 telescope: *a* – the original image; *b* – the generated typical image; *c* – analytical image model

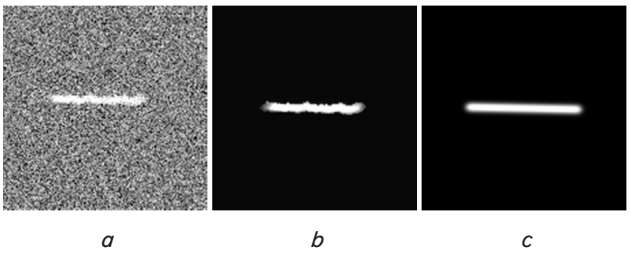

a *b* *c*

Fig. 3. Fragment of the frame of the AZT8 telescope: *a* – the original image; *b* – the generated typical image; *c* – analytical image model

To evaluate the effectiveness of the matched filters, the signal-to-noise ratio (SNR) on frames was calculated after matched filtering with analytical and non-analytical image form. The SNR Q_{nj} for the j-th image of the object on the nth frame was calculated according to the expression:

$$q_{nj} = \frac{A_{nj\,\max}}{k_n \cdot \sigma_{n\,noise}}, \quad (14)$$

where $A_{nj\max}$ is the maximum brightness of the pixel of the j-th object on the nth frame after matched filtering;

$k_n = \sqrt{\frac{1}{N_x N_y} \sum_{u=0}^{Nx-1} \sum_{v=0}^{Ny-1} \left| H_{FM\,uv} \right|^2}$ – the conversion factor of the RMS background substrate of the nth frame after matched filtering;

H_{FMuv} is the value of the uv coefficient of the transfer function of the matched filter;

$u = 0, N_x - 1,\ v = 0, N_y - 1$ – harmonic numbers of the spectrum of the rectangular region of the typical image of the digital frame;

$\sigma_{n\,noise}$ is the RMS of the background substrate of the nth frame.

Table 1 gives the quintiles of the signal-to-noise ratio distribution on images of objects on test frame series after matched filtering with analytical and non-analytical typical form of object images.

Fig. 5–8 show histograms of the relative frequencies of the signal-to-noise ratio on the frames of the series after matched filtering with the analytical (orange translucent) and non-analytical (blue translucent) typical image form.

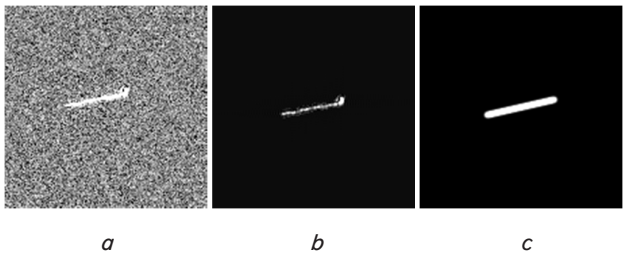

a *b* *c*

Fig. 4. Fragment of the frame of the telescope Takahashi BRC-250M: *a* – the original image; *b* – the generated typical image; *c* – analytical image model

Table 1

Quantiles of signal-to-noise ratios on series frames

Series frames	Matched filter type	SNR quintiles on a series of frames				
		0.025	0.25	0.5	0.75	0.975
QOS «Sazhen S»	Analytical	4.07	11.66	20.83	40.69	104.6
	Non-analytic	3.94	14.54	33.98	61.53	172.23
OMT-800	Analytical	3.52	12.26	25.73	50.4	108.35
	Non-analytic	3.79	13.91	26.78	54.91	138.6
AZT8	Analytical	4.71	19.45	41.15	79.22	218.3
	Non-analytic	4.45	18.64	42.29	91.0	253.91
Takahashi BRC-250M	Analytical	3.3	6.84	12.51	22.48	52.7
	Non-analytic	3.69	10.02	19.77	37.2	101.25

The indicators in Table 1, as well as histograms of the relative frequencies of the signal-to-noise ratio in Fig. 5–8, indicate the successful application of the devised computational method.

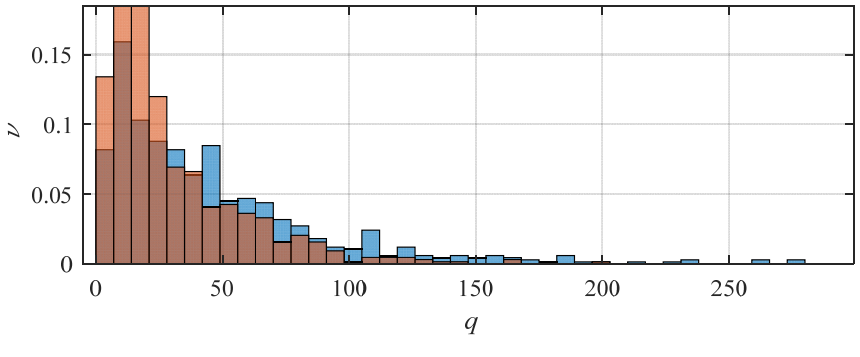

Fig. 5. Signal-to-noise ratio histogram on the frames of the "Sazhen-S" series after matched filtering

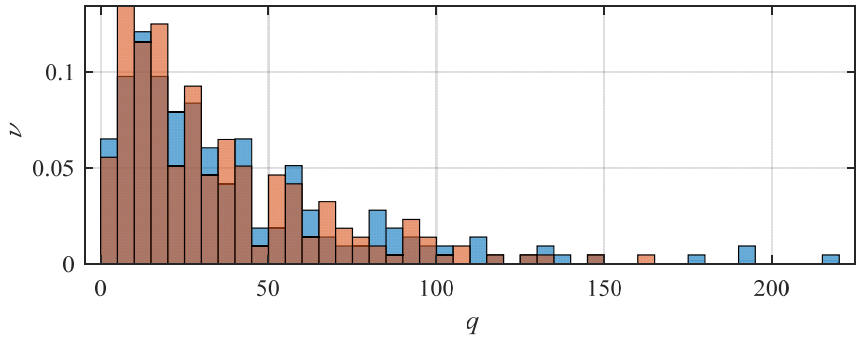

Fig. 6. Signal-to-noise ratio histogram on OMT-800 series frames after matched filtering

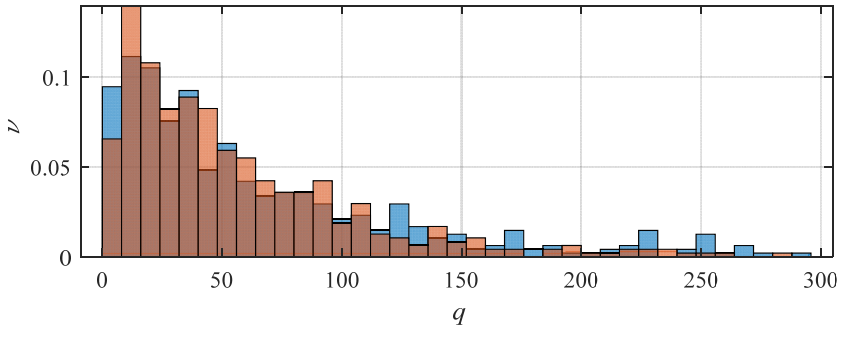

Fig. 7. Signal-to-noise ratio histogram on AZT8 series frames after matched filtering

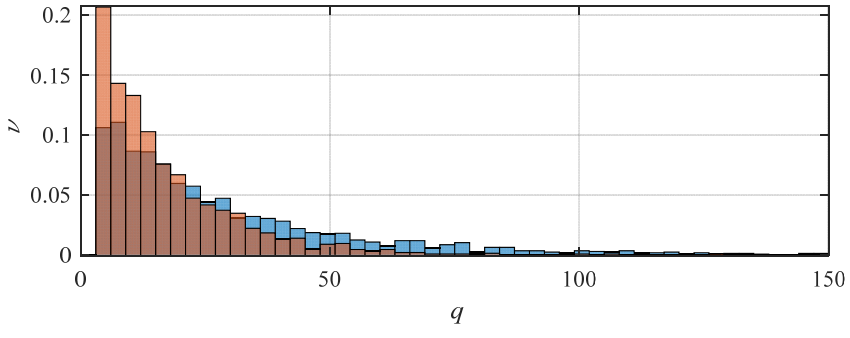

Fig. 8. Signal-to-noise ratio histogram on Takahashi BRC-250M series frames after matched filtering

6. Discussion of the results of studying the matched filtering of a blurred image using its typical form

The possibility of processing blurred digital images of objects on a series of frames was investigated. In the process, typical conditions for the appearance of such blurred images were investigated (Fig. 1–4, *a*). Existing methods of basic image processing and machine vision were also analyzed [12]. However, the accuracy and quality of processing by existing techniques directly depended on the accuracy and quality of the original image of the object itself on a series of frames.

Therefore, in order to develop a procedure for the matched filtering of a blurred digital image, it was proposed to use an automated formation of a standard image shape form instead of the classical use of an analytical form [27].

Within the framework of the CoLiTec project [39], studies were conducted on the application of the devised procedure of matched filtering. As the study showed, after the application of matched filtering, images of cataloged (reference) objects [4] in 92 % of cases began to clearly demonstrate only one brightness peak (Fig. 6, 7). This significantly affects the quality and accuracy of a number of tasks of data acquisition [40], image processing, and machine vision [16]. Also, the use of the devised procedure allows us to reduce the number of false detections due to the formation of a clearer typical shape of the image of the object. This indicator clearly indicates that the tasks set have been successfully completed.

These results are determined by the formation and refinement of the typical shape of the blurred image of the object based on the frames of the entire series. And also, defining the transfer function of the filtered matched filter as the reverse DPF [41] of its spectrum (12).

The limitation of this study is the variety of typical shapes of images of objects due to unfavorable shooting conditions, which leads to variability of the typical shape from frame to frame. Also, a limitation is the computing power of the equipment involved in the processing. The issue of security [42] of frames, namely encryption of input data, is also important. In this case, an additional decryption algorithm will be required before using the method devised.

The disadvantage of the study is precisely the fact that the application of the devised method is impossible immediately after receiving the first frame of the series. This means that the standard shape is based on the data on all images of the same object on each frame of the series. This leads to the fact that the series of frames must be formed completely before applying our method. And this leads to a delay in processing and to idle computing power.

Further research should be concentrated on the application of the devised method of matched filtering as a pre-treatment before the main task of image processing. To this end, it is necessary to use the method/service sampling procedure for the processing pipeline [43]. It is also necessary to evaluate the quantitative and qualitative indicators of the main processing methods that will be used in the future. To do this, it is also possible to analyze (including machine learning [16], Wavelet analysis [44], forecasting procedure [45] and time series analysis [20]) the effect of matched filtering on the basic image processing methods.

7. Conclusions

1. On a series of blurred images, a selection of single images of objects on each frame of the series was made. For each image, image parameters such as eccentricity ε_m, length L_m and the criterion of distortion by coma σ_{Gm} were calculated. Based on these parameters, defective single object images were filtered out and excluded from the list. For the remaining single images of objects, rectangular areas were formed, which made it possible to perform the most accurate assessment of their displacement. The calculations performed have made it possible to carry out normalization, which is necessary to eliminate the differences between the median and aperture (PSF) brightness of the images of objects.

2. For the blurred image of the object, a typical form was formed, which made it possible to determine the coordinates x_{cimg}, y_{cimg} of the reference center. Also, the obtained typical form of the blurred image of the object on each frame of the series was refined. Refinement was achieved by calculating the linear correlation coefficients of the normalized selected single images of objects.

3. To more accurately estimate the initial approximation of the Gaussian shape parameters for the blurred image of the object, their number was determined. It is calculated by dividing the image into N_{segj} segments Δx_{seg} pixels wide along the semi-major axis of the image itself.

4. To prepare a matched filtering of blurred images, the shape and special parameters of the matched filter transfer function were selected. Based on them, the transfer function H_{MF} of the matched filter was built. An OLS-evaluation of the blurred digital image parameters was also carried out.

5. Owing to preliminary calculations, a procedure for the matched filtering of a blurred digital image of the object using its typical form on a series of frames was devised. The use of matched filtering for a blurred image in 94 % of cases allows only one brightness peak to be clearly identified. This also significantly affects the quality and accuracy (an improvement of 20–25 %) of the subsequent execution of a number of image processing and machine vision tasks. Our studies, when comparing the use of an analytical image model and a calculated typical form, have shown a significant advantage of using a typical form (up to 72 %).

Conflicts of interest

The authors declare that they have no conflicts of interest in relation to the current study, including financial, personal, authorship, or any other, that could affect the study and the results reported in this paper.

Funding

The study was conducted without financial support.

Data availability

All data are available in the main text of the manuscript.

References

1. Dearborn, D. P. S., Miller, P. L. (2014). Defending Against Asteroids and Comets. Handbook of Cosmic Hazards and Planetary Defense, 1–18. doi: https://doi.org/10.1007/978-3-319-02847-7_59-1
2. Mykhailova, L., Savanevych, V., Sokovikova, N., Bezkrovniy, M., Khlamov, S., Pogorelov, A. (2014). Method of maximum likelihood estimation of compact group objects location on CCD-frame. Eastern-European Journal of Enterprise Technologies, 5 (4 (71)), 16–21. doi: https://doi.org/10.15587/1729-4061.2014.28028
3. Savanevych, V. E., Khlamov, S. V., Akhmetov, V. S., Briukhovetskyi, A. B., Vlasenko, V. P., Dikov, E. N. et al. (2022). CoLiTecVS software for the automated reduction of photometric observations in CCD-frames. Astronomy and Computing, 40, 100605. doi: https://doi.org/10.1016/j.ascom.2022.100605
4. Akhmetov, V., Khlamov, S., Dmytrenko, A. (2018). Fast Coordinate Cross-Match Tool for Large Astronomical Catalogue. Advances in Intelligent Systems and Computing III, 3–16. doi: https://doi.org/10.1007/978-3-030-01069-0_1
5. Vavilova, I., Pakuliak, L., Babyk, I., Elyiv, A., Dobrycheva, D., Melnyk, O. (2020). Surveys, Catalogues, Databases, and Archives of Astronomical Data. Knowledge Discovery in Big Data from Astronomy and Earth Observation, 57–102. doi: https://doi.org/10.1016/b978-0-12-819154-5.00015-1
6. Cavuoti, S., Brescia, M., Longo, G. (2012). Data mining and knowledge discovery resources for astronomy in the web 2.0 age. Software and Cyberinfrastructure for Astronomy II. doi: https://doi.org/10.1117/12.925321
7. Chalyi, S., Levykin, I., Biziuk, A., Vovk, A., Bogatov, I. (2020). Development of the technology for changing the sequence of access to shared resources of business processes for process management support. Eastern-European Journal of Enterprise Technologies, 2 (3 (104)), 22–29. doi: https://doi.org/10.15587/1729-4061.2020.198527
8. Khlamov, S., Savanevych, V. (2020). Big Astronomical Datasets and Discovery of New Celestial Bodies in the Solar System in Automated Mode by the CoLiTec Software. Knowledge Discovery in Big Data from Astronomy and Earth Observation, 331–345. doi: https://doi.org/10.1016/b978-0-12-819154-5.00030-8
9. Smith, G. E. (2010). Nobel Lecture: The invention and early history of the CCD. Reviews of Modern Physics, 82 (3), 2307–2312. doi: https://doi.org/10.1103/revmodphys.82.2307
10. Khlamov, S., Savanevych, V., Briukhovetskyi, O., Oryshych, S. (2016). Development of computational method for detection of the object's near-zero apparent motion on the series of ccd-frames. Eastern-European Journal of Enterprise Technologies, 2 (9 (80)), 41–48. doi: https://doi.org/10.15587/1729-4061.2016.65999
11. Kuz'min, S. Z. (2000). Tsifrovaya radiolokatsiya. Vvedenie v teoriyu. Kyiv: Izdatel'stvo KviTS, 428.
12. Klette, R. (2014). Concise computer vision. An Introduction into Theory and Algorithms. Springer, 429. doi: https://doi.org/10.1007/978-1-4471-6320-6
13. Kirichenko, L., Zinchenko, P., Radivilova, T. (2020). Classification of Time Realizations Using Machine Learning Recognition of Recurrence Plots. Lecture Notes in Computational Intelligence and Decision Making, 687–696. doi: https://doi.org/10.1007/978-3-030-54215-3_44
14. Akhmetov, V., Khlamov, S., Khramtsov, V., Dmytrenko, A. (2019). Astrometric Reduction of the Wide-Field Images. Advances in Intelligent Systems and Computing, 896–909. doi: https://doi.org/10.1007/978-3-030-33695-0_58

15. Belov, L. A. (2021). Radioelektronika. Formirovanie stabil'nykh chastot i signalov. Moscow: Izdatel'stvo Yurayt, 268.
16. Bishop, C. M. (2013). Model-based machine learning. Philosophical Transactions of the Royal Society A: Mathematical, Physical and Engineering Sciences, 371 (1984), 20120222. doi: https://doi.org/10.1098/rsta.2012.0222
17. Akhmetov, V., Khlamov, S., Tabakova, I., Hernandez, W., Nieto Hipolito, J. I., Fedorov, P. (2019). New approach for pixelization of big astronomical data for machine vision purpose. 2019 IEEE 28th International Symposium on Industrial Electronics (ISIE). doi: https://doi.org/10.1109/isie.2019.8781270
18. Minaee, S., Boykov, Y. Y., Porikli, F., Plaza, A. J., Kehtarnavaz, N., Terzopoulos, D. (2021). Image Segmentation Using Deep Learning: A Survey. IEEE Transactions on Pattern Analysis and Machine Intelligence, 44 (7). doi: https://doi.org/10.1109/tpami.2021.3059968
19. Dadkhah, M., Lyashenko, V. V., Deineko, Z. V., Shamshirband, S., Jazi, M. D. (2019). Methodology of wavelet analysis in research of dynamics of phishing attacks. International Journal of Advanced Intelligence Paradigms, 12 (3/4), 220. doi: https://doi.org/10.1504/ijaip.2019.098561
20. Kirichenko, L., Saif, A., Radivilova, T. (2020). Generalized Approach to Analysis of Multifractal Properties from Short Time Series. International Journal of Advanced Computer Science and Applications, 11 (5). doi: https://doi.org/10.14569/ijacsa.2020.0110527
21. Burger, W., Burge, M. (2010). Principles of digital image processing: core algorithms. Springer, 332. doi: https://doi.org/10.1007/978-1-84800-195-4
22. Steger, C., Ulrich, M., Wiedemann, C. (2018). Machine vision algorithms and applications. John Wiley & Sons, 516.
23. Soyfer, V. A. (Ed.) (2003). Metody komp'yuternoy obrabotki izobrazheniy. Moscow: Fizmatlit, 784.
24. Rubin, B. (2015). Introduction to Radon transforms. With Elements of Fractional Calculus and Harmonic Analysis. Encyclopedia of Mathematics and its Applications. Cambridge University Press, 596.
25. Wang, J., Cai, D., Wen, Y. (2011). Comparison of matched filter and dechirp processing used in Linear Frequency Modulation. 2011 IEEE 2nd International Conference on Computing, Control and Industrial Engineering. doi: https://doi.org/10.1109/ccieng.2011.6008069
26. Jorgensen, B. (2012). Statistical properties of the generalized inverse Gaussian distribution. Springer, 188. doi: https://doi.org/10.1007/978-1-4612-5698-4
27. Khlamov, S., Vlasenko, V., Savanevych, V., Briukhovetskyi, O., Trunova, T., Chelombitko, V., Tabakova, I. (2022). Development of computational method for matched filtration with analytical profile of the blurred digital image. Eastern-European Journal of Enterprise Technologies, 5 (4 (119)), 24–32. doi: https://doi.org/10.15587/1729-4061.2022.26530
28. Savanevych, V., Khlamov, S., Vlasenko, V., Deineko, Z., Briukhovetskyi, O., Tabakova, I., Trunova, T. (2022). Formation of a typical form of an object image in a series of digital frames. Eastern-European Journal of Enterprise Technologies, 6 (2 (120)), 51–59. doi: https://doi.org/10.15587/1729-4061.2022.266988
29. Lemur software. CoLiTec. Available at: https://colitec.space/
30. Khlamov, S., Savanevych, V., Briukhovetskyi, O., Pohorelov, A., Vlasenko, V., Dikov, E. (2018). CoLiTec Software for the Astronomical Data Sets Processing. 2018 IEEE Second International Conference on Data Stream Mining & Processing (DSMP). doi: https://doi.org/10.1109/dsmp.2018.8478504
31. Kashuba, S., Tsvetkov, M., Bazyey, N., Isaeva, E., Golovnia, V. (2018). The Simeiz plate collection of the ODESSA astronomical observatory. Proceedings of the XI Bulgarian-Serbian Astronomical Conference, 207–216.
32. Parimucha, Š., Savanevych, V. E., Briukhovetskyi, O. B., Khlamov, S. V., Pohorelov, A. V., Vlasenko, V. P. et al. (2019). CoLiTecVS - A new tool for an automated reduction of photometric observations. Contributions of the Astronomical Observatory Skalnate Pleso, 49 (2), 151–153. Available at: https://www.ta3.sk/caosp/Eedition/FullTexts/vol49no2/pp151-153.pdf
33. Mingmuang, Y., Tummuangpak, P., Asanok, K., Jaroenjittichai, P. (2019). The mass distribution and the rotation curve of the Milky Way Galaxy using NARIT 4.5 m small radio telescope and the 2.3 m Onsala radio telescope. Journal of Physics: Conference Series, 1380 (1), 012028. doi: https://doi.org/10.1088/1742-6596/1380/1/012028
34. Sergienko, A. B. (2011). Tsifrovaya obrabotka signalov. Sankt-Peterburg: BKhV-Peterburg, 768.
35. Kobzar', A. I. (2006). Prikladnaya matematicheskaya statistika. Dlya inzhenerov i nauchnykh rabotnikov. Moscow: FIZMATLI, 816.
36. Le, D.-H., Pham, C.-K., Nguyen, T. T. T., Bui, T. T. (2012). Parameter extraction and optimization using Levenberg-Marquardt algorithm. 2012 Fourth International Conference on Communications and Electronics (ICCE). doi: https://doi.org/10.1109/cce.2012.6315945
37. Gonzalez, R., Woods, R. (2018). Digital image processing. New York, NY: Pearson, 1168.
38. Ivanov, M. T., Sergienko, A. B., Ushakov, V. N. (2021). Radiotekhnicheskie tsepi i signaly. Sankt-Peterburg: Piter, 336.

39. Khlamov, S., Savanevych, V., Briukhovetskyi, O., Tabakova, I., Trunova, T. (2022). Data Mining of the Astronomical Images by the CoLiTec Software. CEUR Workshop Proceedings, 3171, 1043–1055.
40. Zhang, Y., Zhao, Y., Cui, C. (2002). Data mining and knowledge discovery in database of astronomy. Progress in Astronomy, 20 (4), 312–323.
41. Rao, K. R., Kim, D. N., Hwang, J.-J. (2010). Fast Fourier Transform - Algorithms and Applications. Springer, 426. doi: https://doi.org/10.1007/978-1-4020-6629-0
42. Buslov, P., Shvedun, V., Streltsov, V. (2018). Modern Tendencies of Data Protection in the Corporate Systems of Information Consolidation. 2018 International Scientific-Practical Conference Problems of Infocommunications. Science and Technology (PIC S&T). doi: https://doi.org/10.1109/infocommst.2018.8632089
43. Petrychenko, A., Levykin, I., Iuriev, I. (2021). Improving a method for selecting information technology services. Eastern-European Journal of Enterprise Technologies, 2 (2 (110)), 32–43. doi: https://doi.org/10.15587/1729-4061.2021.229983
44. Baranova, V., Zeleniy, O., Deineko, Z., Bielcheva, G., Lyashenko, V. (2019). Wavelet Coherence as a Tool for Studying of Economic Dynamics in Infocommunication Systems. 2019 IEEE International Scientific-Practical Conference Problems of Infocommunications, Science and Technology (PIC S&T). doi: https://doi.org/10.1109/picst47496.2019.9061301
45. Dombrovska, S., Shvedun, V., Streltsov, V., Husarov, K. (2018). The prospects of integration of the advertising market of Ukraine into the global advertising business. Problems and Perspectives in Management, 16 (2), 321–330. doi: https://doi.org/10.21511/ppm.16(2).2018.29